Corundum and hercynite in bauxite from South Western Australia

Robert Gilkes[1], Saowanuch Tawornpruek[2] and Nattaporn Prakongkep[1]

[1]School of Earth and Environment, Faculty of Natural and Agricultural Sciences, University of Western Australia, Crawley, WA 6009, Australia[bob.gilkes@uwa.edu.au]
[2]Department of Soil Science, Faculty of Agriculture, Kasetsart University, Bangkok 10900, Thailand

Introduction

Boddington bauxite from the Darling Range lateritic bauxite province in south-western Australia has formed from diverse granitic and mafic parent rocks. The bauxite profile contains saprock, saprolite, pallid clay, B-zone ore, hardcaps and gravel (Ball and Gilkes, 1987). The mined bauxite represents a mixture of B-zone, hardcap and gravel with a mineralogy dominated by gibbsite, goethite, hematite and quartz. Minor constituents include boehmite, corundum, maghemite, anatase, kaolin and muscovite together with diverse resistant sand-size primary mineral grains (zircon, monazite, etc). Extraction of Al from this bauxite using the Bayer process varies in efficiency with the type of bauxite being processed and in particular with the mineralogy of the bauxite. This paper identifies forms of Al that are not dissolved during Bayer process extraction and which are partly responsible for differences in extraction efficiency between bauxite materials. Hercynite, corundum and poorly ordered alumina occur in Darling Range bauxite and have been characterized using conventional and synchrotron X-ray diffraction and high resolution analytical electron microscopy (EDS, EELS, SAD, HRTEM).

Materials and Methods

Samples of gravel, caprock and B-grade bauxite from the Boddington mine and residues of these materials after caustic digestion were examined. Caustic digestion treatment removed gibbsite and kaolinite and concentrated iron oxides and other minerals. Iron oxides were removed from the samples by DCB (dithionite-citrate-bicarbonate) treatment (Mehra and Jackson, 1960). Maghemite was separated by magnetic separation (MAG) and quartz was removed from the concentrates by sedimentation and sometimes heavy liquid separation.

For random powder X-ray diffraction (XRD) measurements, mineral concentrate samples were scanned from 4 to 65° 2θ, using a step size of 0.02° 2θ and a scan speed of 0.004° 2θ sec^{-1} (Brown and Brindley, 1980) with a Philips PW-3020 diffractometer using CuKα radiation and a graphite monochromator.

XRD patterns of the mineral concentrate samples were also obtained using synchrotron radiation on the Australian synchrotron. Powdered mineral concentrate samples were placed in glass capillaries, and analyzed over an angular range of 4–60° 2θ. The wavelength was set at ~0.1 nm to provide for adequate dispersion/resolution.

The TEM specimens were prepared using the clay fraction which was ultrasonically dispersed in ultrapure water and a few drops of the suspension were deposited on a copper grid covered with a holey carbon film. TEM-EDS (transmission electron microscopy with energy dispersive analysis of X-rays), EFTEM (energy filtered transmission electron microscopy), SAD (selected area diffraction) and high resolution transmission electron microscopy (HRTEM) data for particles were obtained with a JEOL 3000F FEGTEM operated at 300 kV to determine the morphology and composition of mostly submicron size particles. A 300 kV JEOL 3000F field-emission TEM equipped with a post-column Gatan Imaging Filter, a TV-rate retractable camera and Multi Scan digital camera (Gatan, Pleasanton, CA) was employed for EFTEM work.

Results

Corundum

Minor amounts of Fe^{3+} are generally associated with corundum crystals as indicated by energy filtered electron micrographs and associated EELS spectra (Figures 1,2). This minor amount of Fe^{3+} (about 1 atom %) is not uniformly distributed throughout crystals and may consist of Fe-oxide particles on the surface and in voids in corundum particles. However the particles shown in Figures 4 and 5 had been extracted with citrate-bicarbonate-dithionite solution to remove free iron oxides so that the Fe indicated by these data is more likely present within the structure of corundum. Such low amounts of Fe substitution did not affect unit cell dimensions.

Hercynite

Hercynite (ideally Al_2FeO_4 – Fe present as Fe^{2+}) was mostly present in gravel and hardcap materials and was never present at amounts greater than 10%. It consists of anhedral granular platey 20-200 nm particles with lattice fringes extending throughout particles that generate Fourier transform diffraction patterns thus indicating that the particles are single crystals (Figure 3). X-ray spectra of hercynite particles indicate that the composition is quite variable and particles often contain more Al than ideal hercynite. EELS spectra show that Fe is present as Fe^{2+} (Figure 4).

Poorly Ordered Aluminas

XRD patterns of caustic residues of some gravel and hardcap samples indicate that poorly ordered gamma and chi aluminas are present in bauxite. These minerals are not dissolved by the Bayer process.

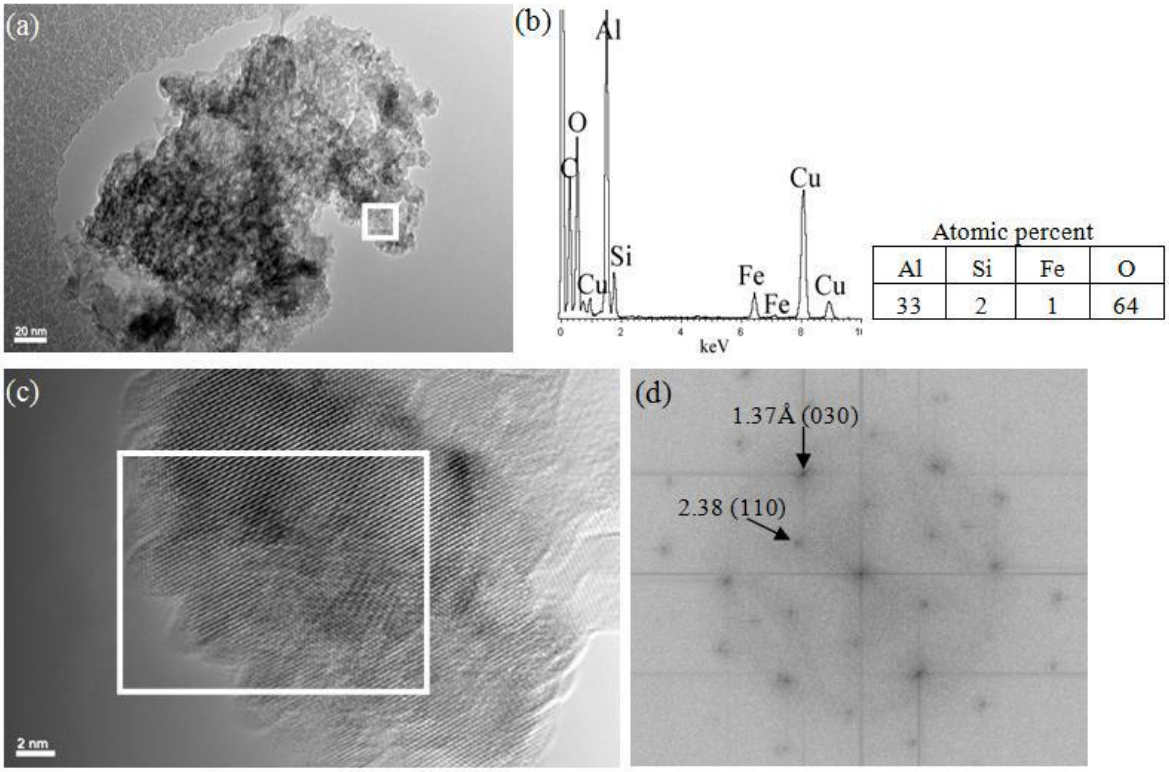

Fig. 1. (a) Electron micrograph of a corundum particle, (b) x-ray spectrum of the particle indicating minor substitution of Fe for Al (The Si and Cu peaks are due to the supporting film and grid respectively), (c) high resolution electron micrograph of the area indicated by the white square in (a) and (d) Fourier transform diffraction pattern of a region of the corundum particle indicated by the white square in (c).

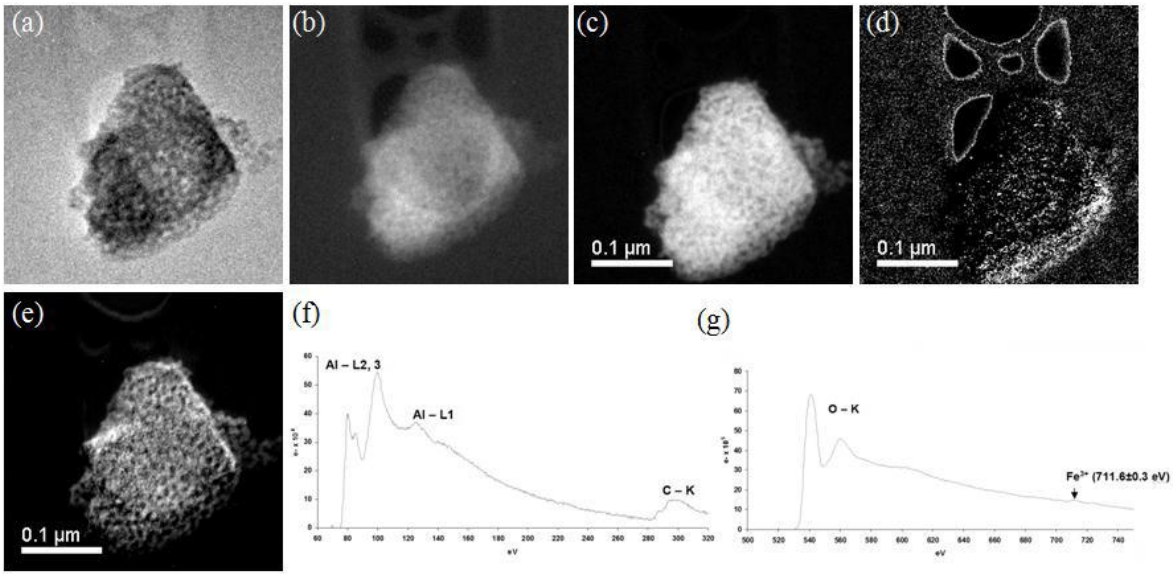

Fig. 2. (a) Energy filtered electron micrograph of a corundum particle, (b) thickness map, (c) oxygen map, (d) iron map, (e) aluminium map, (f) EELS for aluminium and carbon, (g) EELS for oxygen and ferric iron.

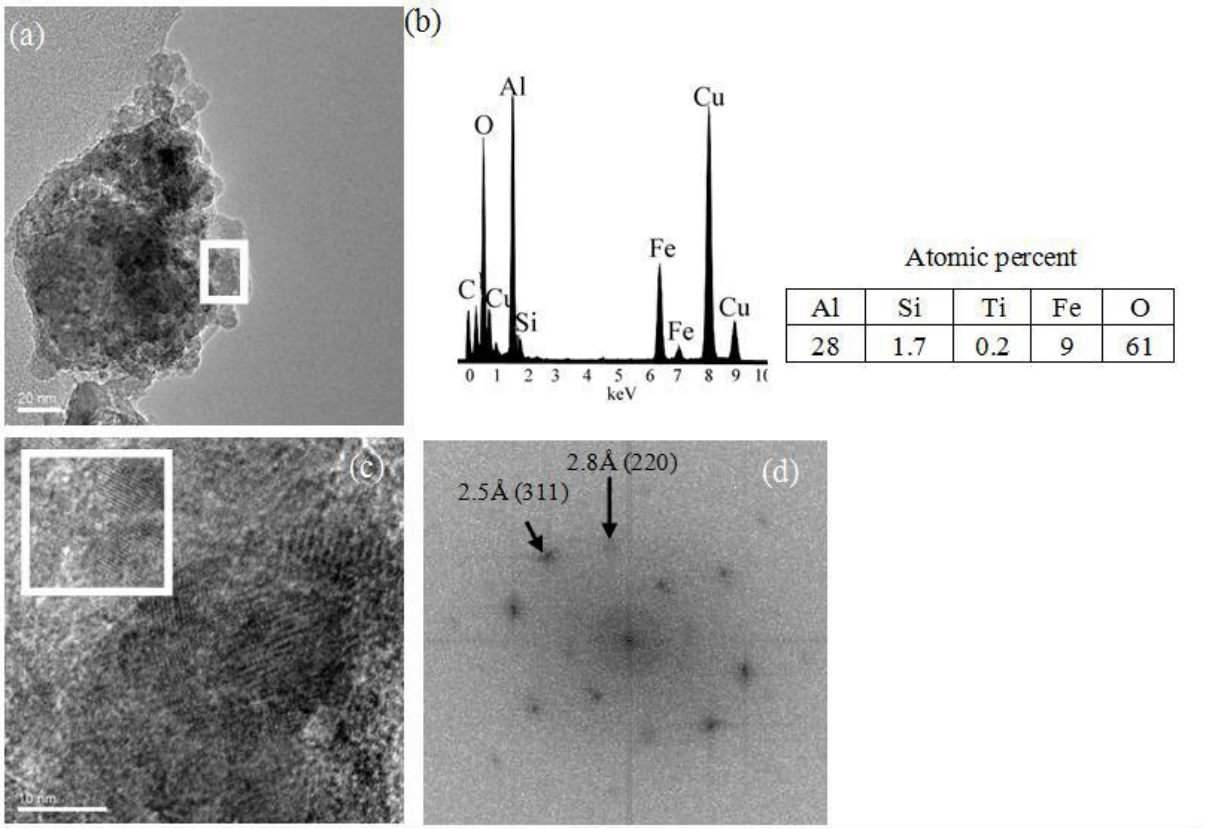

Al	Si	Ti	Fe	O
28	1.7	0.2	9	61

Fig. 3. (a) Electron micrograph of a hercynite particle, (b) x-ray spectrum of the particle. (The Si and Cu peaks are due to the supporting film and grid respectively.) (c) high resolution electron micrograph of the indicated area of the particle showing a lattice image and (d) Fourier transform diffraction pattern for the indicated area in (c).

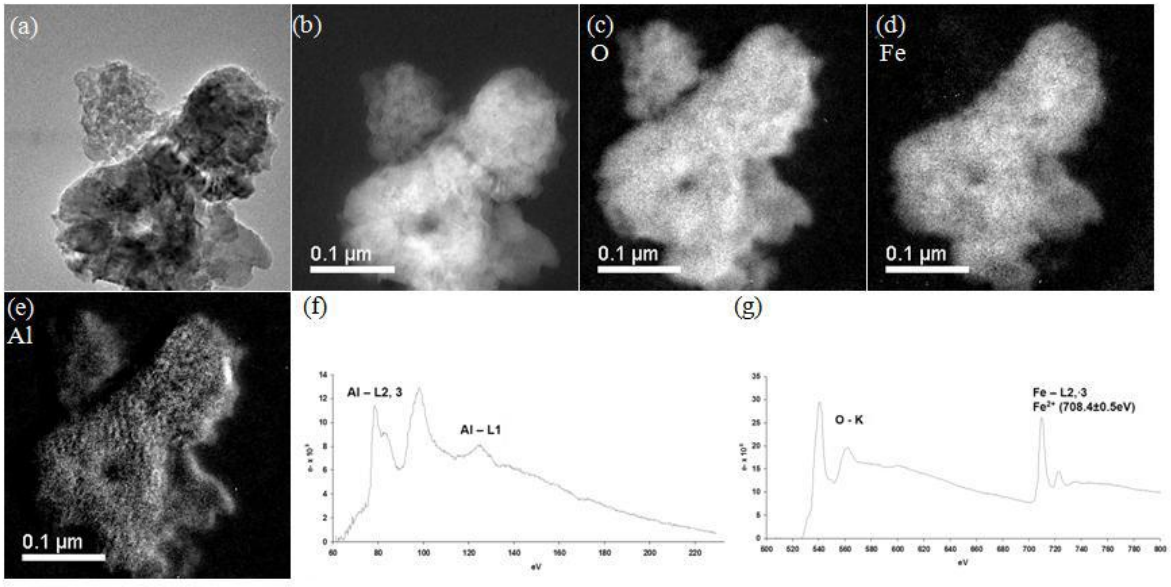

Fig. 4. (a) Energy filtered electron micrographs of the hercynite particles, (b) thickness map, (c) oxygen map, (d) iron map, (e) aluminium map, (f) EELS for aluminium and (g) EELS for oxygen and iron which corresponds to ferrous (Fe^{2+}).

Conclusion

This XRD and electron optical examination of residues of caustic and other extractions of diverse bauxite materials from the Boddington bauxite deposit has identified several Al-containing minerals that comprise the non-available Al in this deposit. This knowledge is valuable to the development of improved ore evaluation and Al extraction procedures.

Acknowledgments

We are grateful to BHP Billiton Worsley Alumina Pty Ltd for providing financial assistance to carry out this work and special thanks to Professor Martin Saunders, Centre of Microscopy, Characterisation and Analysis, The University of Western Australia for their excellent TEM technique support. We thank the Australian Synchrotron for beamtime and for technical assistance.

References

Ball P.J. and R.J. Gilkes. 1987. The Mount Saddleback bauxite deposit, Southwestern Australia. Chemical Geology 60: 215-225 215.

Brown, G. and G.W. Brindley. 1980. X-ray diffraction procedures for clay mineral identification, pp. 305-359. In G.W. Brindley and G. Brown, eds. Crystal Structures of Clay Minerals and Their X-ray Identification. Mineralogical Society, London.

Mehra, O. and P. Jackson. 1960. Iron oxide removal from soils and clays in a dithionite-citrate-bicarbonate system buffered with sodium bicarbonate. Clays Clay Miner. 7: 317-327

Notes